



TRANSLATIONAL SCIENCE

Combined genetic analysis of juvenile idiopathic arthritis clinical subtypes identifies novel risk loci, target genes and key regulatory mechanisms

Elena López-Isac ,¹ Samantha L Smith ,¹ Miranda C Marion,² Abigail Wood,¹ Marc Sudman,³ Annie Yarwood ,¹ Chenfu Shi,¹ Vasanthi Priyadarshini Gaddi,¹ Paul Martin ,^{1,4} Sampath Prahalad ,⁵ Stephen Eyre,^{1,6} Gisela Orozco,^{1,6} Andrew P Morris,¹ Carl D Langefeld,² Susan D Thompson,³ Wendy Thomson,^{1,6} John Bowes ,^{1,6}

Handling editor Josef S Smolen

For numbered affiliations see end of article.

Correspondence to

Dr John Bowes, Centre for Genetics and Genomics Versus Arthritis, Centre for Musculoskeletal Research, Manchester Academic Health Science Centre, The University of Manchester, Manchester, UK; j.bowes@manchester.ac.uk

WT and JB contributed equally.

Received 1 July 2020

Revised 28 August 2020

Accepted 16 September 2020

Published Online First

26 October 2020

ABSTRACT

Objectives Juvenile idiopathic arthritis (JIA) is the most prevalent form of juvenile rheumatic disease. Our understanding of the genetic risk factors for this disease is limited due to low disease prevalence and extensive clinical heterogeneity. The objective of this research is to identify novel JIA susceptibility variants and link these variants to target genes, which is essential to facilitate the translation of genetic discoveries to clinical benefit.

Methods We performed a genome-wide association study (GWAS) in 3305 patients and 9196 healthy controls, and used a Bayesian model selection approach to systematically investigate specificity and sharing of associated loci across JIA clinical subtypes. Suggestive signals were followed-up for meta-analysis with a previous GWAS (2751 cases/15 886 controls). We tested for enrichment of association signals in a broad range of functional annotations, and integrated statistical fine-mapping and experimental data to identify target genes.

Results Our analysis provides evidence to support joint analysis of all JIA subtypes with the identification of five novel significant loci. Fine-mapping nominated causal single nucleotide polymorphisms with posterior inclusion probabilities $\geq 50\%$ in five JIA loci. Enrichment analysis identified RELA and EBF1 as key transcription factors contributing to disease risk. Our integrative approach provided compelling evidence to prioritise target genes at six loci, highlighting mechanistic insights for the disease biology and *IL6ST* as a potential drug target.

Conclusions In a large JIA GWAS, we identify five novel risk loci and describe potential function of JIA association signals that will be informative for future experimental works and therapeutic strategies.

Key messages

What is already known about this subject?

- Juvenile idiopathic arthritis (JIA) is the most common form of childhood arthritis. However, our understanding of the genetic basis of JIA is hampered by low disease prevalence and extensive clinical heterogeneity represented by seven disease subtypes, with only 17 known susceptibility loci to date.

What does this study add?

- Although JIA is a heterogeneous disease, we show that most susceptibility loci are shared across multiple clinical subtypes, enabling joint analysis of clinically related subtypes, both for this study and future projects, increasing the power of our study leading to the identification of five novel susceptibility loci in the largest genome-wide genetic study to date.
- By linking susceptibility genetic variants to target genes, integrating functional annotations, statistical fine mapping, expression data from 15 immunological cell types and chromatin interaction data (HiChIP and Hi-C) from human T and B cell types, we identify putative causal (i) single nucleotide polymorphisms; (ii) genes and (iii) cell types while also highlighting key regulatory mechanisms underlying disease.

heterogeneous forms of childhood arthritis that are clinically encompassed under the term of juvenile idiopathic arthritis (JIA). JIA comprises childhood rheumatic conditions characterised by inflammatory arthritis of unknown origin that persists for at least 6 weeks and begins before the age of 16 years.³

The International League of Associations for Rheumatology (ILAR) distinguishes seven JIA subtypes: oligoarticular arthritis (oligoJIA); rheumatoid factor (RF)-negative polyarthritis (RF-polyJIA); RF-positive polyarthritis (RF+polyJIA); juvenile psoriatic arthritis (JPsA); enthesitis-related arthritis; childhood spondyloarthropathy (ERA); systemic arthritis (sJIA); and undifferentiated arthritis.⁴

To date genetic studies in JIA susceptibility have identified 17 genome-wide significant associations



© Author(s) (or their employer(s)) 2021. Re-use permitted under CC BY. Published by BMJ.

To cite: López-Isac E, Smith SL, Marion MC, et al. Ann Rheum Dis 2021;80:321–328.

Key messages

How might this impact on clinical practice or future developments?

- The results of this study demonstrate that clinically heterogeneous subtypes can be analysed in a combined approach to identify novel shared susceptibility loci which is an approach that will be informative for genetic studies of other clinically heterogeneous diseases.
- We identify causal genes at JIA susceptibility loci which is an essential step in the translational of genetic discoveries to clinical benefit by highlighting potential therapeutic targets.

highlighting a number of key findings^{5–7} including, first, that there is overlap of susceptibility loci between two of the most common JIA subtypes, oligoJIA and RF-polyJIA; specifically, in the human leucocyte antigen (HLA) region, these two subtypes share the presence of a glycine at amino acid position 13 of HLA-DRB1 as their highest risk factor, resembling the findings in adult seronegative rheumatoid arthritis (RA).^{6,7} Together these two JIA subtypes define a genetically homogeneous cluster sometimes referred to with the term ‘polygo’.^{7–9} Second, this high genetic correlation is not as evident in the remaining subtypes, especially considering their divergent associations observed across the HLA region. For example, the presence of a histidine at the same HLA-DRB1 position confers the highest risk for RF+polyJIA, consistent with the association reported in adult seropositive RA.⁷ In addition, the amino acid at position 58 of HLA-DRB1 has been shown to be a specific risk factor for sJIA.¹⁰

The clinical heterogeneity of JIA remains a challenging issue in deciphering its genetic architecture by balancing the need to focus on more clinically/genetically homogeneous subtypes against potentially sacrificing sample size. As a result, there has been a tendency to address the genetics of JIA in a subtype-based manner.^{6–9} However, multinomial approaches have recently been developed to overcome the heterogeneity problem by allowing exploration of the genetic relationships between multi-phenotype categories.¹¹ In this study, we hypothesised that a genome-wide association study (GWAS) combining all JIA subtypes would optimise the success rate in locus discovery. We, therefore, performed a new genome-wide scan of ~7.5 million single nucleotide polymorphisms (SNPs) in the largest JIA GWAS cohort recruited to date, and implemented a novel approach to systematically investigate specificity and sharing of associated loci across ILAR subtypes to support our strategy.

METHODS

Study cohort and GWAS quality control

A total of 4520 UK JIA samples and 9965 healthy individuals were recruited for the present study. JIA DNA samples were genotyped on the Illumina Infinium CoreExome and Infinium OmniExpress genotyping arrays. Sample-level quality control (QC) was applied based on the following exclusion criteria: call rate <0.98 and discrepancy between genetically inferred sex and database records. SNPs that were non-autosomal, had a call rate <0.98 or a minor allele frequency (MAF) <0.01 were excluded. Healthy controls were genotyped using the Illumina Infinium CoreExome genotyping array. QC was consistent with that described above for JIA samples.

Identity-by-descent was used to identify related individuals across all study samples. For each related pair, the sample with the highest call rate was retained. Outliers were identified and

excluded based on ancestry using principal component (PC) analysis performed with the flashpca software package (V2.0) where outliers were identified using aberrant R library (V1.0).^{12,13}

The total number of individuals that remained in the final QC-filtered data set was 12 501 (3305 cases and 9196 healthy controls) (online supplemental table 1).

Imputation

The QC-filtered GWAS data set was subjected to whole-genome genotype imputation. Haplotype phasing and imputation were performed in the Michigan Imputation server using SHAPEIT2¹⁴ and Minimac3,¹⁵ respectively, and the Haplotype Reference Consortium reference panel. Following imputation, SNPs were excluded based on MAF <0.01 and imputation quality (r^2) <0.4.

Association testing and meta-analysis

Case-control association testing was performed by SNPTEST software package (V2.5.2). Three PCs were included as covariates to account for any residual population substructure. Any SNP with a p value <5 × 10⁻⁶ was selected for validation in GWAS summary statistics from an independent data set of 2751 JIA cases (oligoJIA and RF-polyJIA) and 15 886 controls of European ancestry.⁸ An inverse variance weighted fixed effects meta-analysis was performed using the software package GWAMA (V2.2.2).¹⁶ The presence of heterogeneity of ORs across data sets was evaluated with the test statistics I² and Q.

Clinical subtype specificity

The specificity and sharing of JIA susceptibility SNPs across ILAR subtypes was interrogated using Bayesian multinomial logistic regression assuming an additive model implemented in the software package Trinculo (V0.96).¹¹ Model selection for specificity or sharing was based on comparison of log-Bayes factors (logBFs) where a positive logBF was interpreted as evidence that a particular association is specific to an ILAR subtypes, and vice versa.

Statistical fine-mapping of JIA-associated loci

Statistical fine-mapping of the association signal within each locus was performed using the FINEMAP software package (V1.3.1).¹⁷ The method estimates the posterior inclusion probabilities (PIPs) for SNPs to be causal, which in turn were used to generate 95% credible SNP sets for each locus (the smallest list of variants that jointly have a probability of including the causal variant ≥95%).

Functional annotation enrichment analysis

Summary statistics from the GWAS including all ILAR subtypes were tested for enrichment in four categories of annotations based on experimental genomic data including gene structure (coding sequence (CDS), 3'UTR and 5'UTR) from the GENCODE Project, binding sites for 165 transcription factors (TFs) from the ENCODE Project, and enhancers and active promoters for 98 cell types derived from the Roadmap Epigenomics Project.^{18–20} Enrichment of JIA associations were tested separately in each annotation using fgwas (V0.3.6).²¹ A joint model of independent enrichments was further identified using the cross-validation likelihood option implemented in fgwas.

Gene prioritisation

Expression quantitative trait locus (eQTL) data for 15 immune cell types was downloaded from the DICE (Database of Immune Cell Expression, eQTLs and Epigenomics) project website.²²

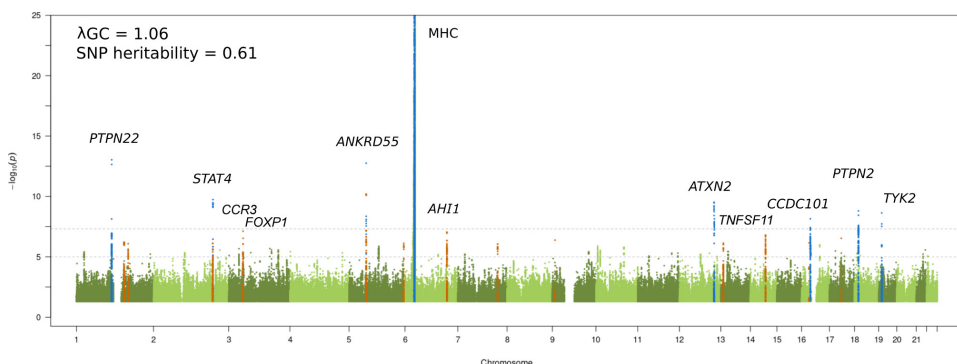


Figure 1 Manhattan plot representing the JIA GWAS results. The $-\log_{10}$ of the p values are plotted against their physical chromosomal position. The upper and lower lines represent the genome-wide significance level ($p \leq 5 \times 10^{-8}$) and p value threshold at $p \leq 1 \times 10^{-6}$, respectively. The plot has been truncated at $p \leq 1 \times 10^{-25}$. Genome-wide significant associations are coloured blue and suggestive significance are coloured orange. Genome-wide significant loci and the suggestive signals that reached $p \leq 5 \times 10^{-8}$ after the replication step are labelled. The genomic inflation factor (λ_{GC}) estimated on the complete data set was 1.06, with a rescaled λ_{1000} of 1.01 indicating minimal residual population stratification based on inflation of test statistics. The SNP-based heritability for JIA susceptibility was estimated to be 0.61 (SE 0.04). JIA, juvenile idiopathic arthritis; GWAS, genome-wide association study; SNP, single nucleotide polymorphism.

Correlation of susceptibility association signals and gene expression were identified by selecting the top eQTL SNP for each gene and retaining those that were also present in the combined list of all credible SNPs. This analysis was further supported by statistical colocalisation of association and eQTL signals. The identification of the target genes of JIA-associated regions was further complemented by the interrogation of high-resolution maps of chromatin interactions for SNPs correlated with eQTL signals using H3K27ac HiChIP data in B and T cells.²³ We also explored chromatin interaction maps obtained by capture Hi-C.²⁴

Additional details of the Methods are available in the online supplemental material.

RESULTS

Five novel susceptibility loci for JIA

We performed a JIA GWAS comprising 12 501 individuals (3305 cases and 9196 healthy controls) and a high-density SNP panel with 7 461 861 variants. The combined analysis of all available JIA cases identified eight loci reaching genome-wide significance ($p \leq 5 \times 10^{-8}$), of which seven have previously been reported and recognised by the notable gene at each locus: MHC (6p25-p34), PTPN22 (1p13.2), STAT4 (2q32.2-q32.3), ANKRD55 (5q11.2), ATXN2 (12q24.12), PTPN2 (18p11.21), and TYK2 (19p13.2) (figure 1 and table 1).⁶ The strongest association was found to SNPs within the extended MHC region (chr6: 28 477 797 to 33 448 354). An in-depth analysis of this region has previously been reported for JIA, including a subset of samples from the current study; therefore this study will focus on non-MHC associations.⁷ The novel genome-wide significant association was represented by the lead SNP rs497523 ($p=7.12 \times 10^{-9}$), which is intronic to CCDC101 (16p11.2), also known as SGF29. A further 37 lead SNPs from independent loci, based on linkage disequilibrium, reached the suggestive significance threshold ($p \leq 5 \times 10^{-6}$). This included previously reported and potentially novel JIA loci (table 1). Summary statistics for 22 of these variants were available from a previously published JIA GWAS comprising 2751 cases and 15 886 controls⁸ and meta-analysed with the current GWAS data. The meta-analysis identified a further four novel SNPs exceeding genome-wide significance in the proximity of the genes AH11 (6q23.3), CCR3 (3p21.31), TNFSF11 (13q14.11) and FOXP1 (3p13) (table 2 and online supplemental table 2). Hence, a total of five new signals associated with JIA were identified. In addition, three SNPs showed

evidence for replication in the independent data set although the meta-analysis test statistic did not exceed genome-wide significance (table 2): TNFSF8 (rs7043505) ($_{meta}p=8.27 \times 10^{-8}$), AAF3 (rs11692867) ($_{meta}p=9.26 \times 10^{-8}$), and RUNX3 (rs72657048) ($_{meta}p=3.51 \times 10^{-7}$). There was no evidence of between-study heterogeneity at any of these loci.

Evidence for shared non-HLA loci across JIA clinical subtypes

We systematically addressed the genetic relationship across ILAR subtypes in a Bayesian framework. We performed a Bayesian model selection between the best subgroup-specific model and the best sharing model and estimated the logBFs for specificity of effects at each locus. The analysis included the 44 non-HLA index SNPs passing study suggestive significance threshold (5×10^{-6}) (table 1). The results revealed evidence for sharing of JIA susceptibility loci across multiple ILAR subtypes since most of the analysed SNPs showed negative logBFs for specificity. This pattern was also evident for previously reported JIA susceptibility SNPs based on a combined cohort of oligoJIA and RF-polyJIA subtypes (online supplemental table 3, online supplemental figure 1). Moreover, the vast majority of the strongest logBFs (values between -4.5 and -9) were observed for the sharing model that comprised all JIA subtypes. Only seven loci (16%) showed weak evidence in favour of them being specific to the polygo subgroup (logBF of 0.06 to 0.5). Overall, these findings support our approach of performing a joint analysis of all available JIA cases to maximise power to detect novel susceptibility loci.

Enrichment of JIA susceptibility SNPs in TFBS and cell-type specific regulatory regions

We investigated the over-representation of JIA susceptibility SNPs in functional categories including gene structure (CDS, 3'UTR and 5'UTR), transcription factor binding sites (TFBSs) and enhancers and active promoters in 98 cell/tissue types. Our results showed no evidence for significant enrichment of JIA susceptibility SNPs in any of the gene structure annotations (p values > 0.1) (figure 2). The most significant enrichment was found to binding sites for the TF RELA (p value $= 2.66 \times 10^{-8}$) (online supplemental table 4 and online supplemental figure 2). Additionally 52 out of the 165 TFBSs interrogated showed significant over-representation, including EBF1 (p value $= 6.00 \times$

Paediatric rheumatology

Table 1 Non-HLA index SNPs passing study suggestive significance threshold (5×10^{-6}) and genome-wide significance threshold

| SNP | Chr. | Position (bp) | Notable genes | Risk/non-risk allele | RAF | HWE (cases) | HWE (controls) | P value | OR | 95% CI |
|-------------|------|---------------|----------------------------|----------------------|------|-------------|----------------|----------|------|--------------|
| rs6679677 | 1 | 114 303 808 | <i>RSBN1; PTPN22</i> | A/C | 0.1 | 0.19 | 0.35 | 9.18E-14 | 1.36 | 1.24 to 1.48 |
| rs7731626 | 5 | 55 444 683 | <i>ANKRD55</i> | G/A | 0.63 | 0.27 | 0.38 | 1.76E-13 | 1.22 | 1.15 to 1.3 |
| rs11889341 | 2 | 191 943 742 | <i>STAT4</i> | T/C | 0.22 | 0.96 | 1 | 1.83E-10 | 1.24 | 1.16 to 1.32 |
| rs4766578 | 12 | 111 904 371 | <i>ATXN2</i> | T/A | 0.49 | 0.21 | 0.13 | 3.03E-10 | 1.22 | 1.15 to 1.29 |
| rs9960807 | 18 | 12 770 851 | <i>RP11-973H7.1; PTPN2</i> | G/A | 0.13 | 0.74 | 0.46 | 1.58E-09 | 1.26 | 1.16 to 1.36 |
| rs34536443 | 19 | 10 463 118 | <i>TYK2</i> | G/C | 0.95 | 0.77 | 0.56 | 2.32E-09 | 1.53 | 1.31 to 1.79 |
| rs497523 | 16 | 28 577 931 | <i>CLN3; CCDC101</i> | T/C | 0.65 | 0.94 | 0.03 | 7.12E-09 | 1.17 | 1.11 to 1.25 |
| rs13160933 | 5 | 55 545 859 | NA | C/T | 0.88 | 0.84 | 1 | 6.49E-08 | 1.26 | 1.15 to 1.38 |
| rs79815064 | 3 | 46 277 577 | <i>CCR3</i> | A/G | 0.87 | 0.45 | 0.6 | 7.61E-08 | 1.25 | 1.14 to 1.37 |
| rs2614258 | 6 | 135 677 202 | <i>AHI1</i> | A/G | 0.38 | 0.2 | 0.22 | 9.17E-08 | 1.15 | 1.08 to 1.22 |
| rs1051533 | 14 | 69 259 662 | <i>ZFP36L1</i> | A/C | 0.21 | 0.63 | 0.85 | 1.62E-07 | 1.2 | 1.12 to 1.28 |
| rs113171555 | 17 | 38 296 272 | <i>CASC3</i> | A/G | 0.02 | 0.73 | 0.14 | 2.92E-07 | 1.46 | 1.22 to 1.75 |
| rs72704368 | 9 | 8 894 396 | <i>PTPRD</i> | A/G | 0.05 | 0.76 | 0.64 | 4.14E-07 | 1.3 | 1.15 to 1.47 |
| rs2481065 | 1 | 154 311 911 | <i>ATP8B2; IL6R</i> | G/A | 0.11 | 0.32 | 0.87 | 6.11E-07 | 1.24 | 1.14 to 1.35 |
| rs77011494 | 16 | 24 333 566 | <i>CACNG3</i> | A/G | 0.04 | 0.86 | 0.89 | 7.04E-07 | 1.41 | 1.23 to 1.6 |
| rs7320806 | 13 | 27 684 929 | <i>USP12</i> | C/A | 0.09 | 0.86 | 0.12 | 7.36E-07 | 1.25 | 1.14 to 1.37 |
| rs6434390 | 2 | 191 262 762 | <i>INPP1; MFSD6</i> | G/C | 0.48 | 0.05 | 0.54 | 7.42E-07 | 1.16 | 1.1 to 1.23 |
| rs12654812 | 5 | 176 794 191 | <i>RGS14</i> | A/G | 0.34 | 0.22 | 0.64 | 7.61E-07 | 1.17 | 1.1 to 1.24 |
| rs840012 | 1 | 167 414 872 | <i>CD247</i> | C/T | 0.59 | 0.46 | 0.95 | 8.21E-07 | 1.15 | 1.08 to 1.22 |
| rs12706860 | 7 | 128 570 026 | NA | C/G | 0.65 | 0.6 | 0.13 | 8.78E-07 | 1.18 | 1.11 to 1.25 |
| rs7204355 | 16 | 58 951 694 | <i>RP11-410D17.2</i> | G/T | 0.79 | 0.26 | 0.07 | 1.04E-06 | 1.19 | 1.1 to 1.28 |
| rs706778 | 10 | 6 098 949 | <i>IL2RA</i> | T/C | 0.4 | 0.34 | 0.78 | 1.28E-06 | 1.15 | 1.09 to 1.22 |
| rs4869314 | 5 | 96 229 225 | <i>ERAP2</i> | G/T | 0.49 | 0.58 | 0.88 | 1.35E-06 | 1.14 | 1.08 to 1.21 |
| rs7082720 | 10 | 90 742 049 | <i>ACTA2</i> | T/C | 0.45 | 0.6 | 0.66 | 1.67E-06 | 1.15 | 1.09 to 1.21 |
| rs2222138 | 18 | 12 889 217 | <i>PTPN2</i> | G/T | 0.68 | 0.42 | 0.98 | 2.02E-06 | 1.17 | 1.1 to 1.24 |
| rs1521088 | 3 | 132 815 094 | <i>TMEM108</i> | T/C | 0.02 | 0.74 | 0.06 | 2.08E-06 | 1.41 | 1.18 to 1.68 |
| rs34173901 | 3 | 33 087 914 | <i>GLB1</i> | C/G | 0.15 | 0.3 | 0.65 | 2.13E-06 | 1.2 | 1.12 to 1.3 |
| rs76870128 | 3 | 138 211 845 | <i>CEP70</i> | C/T | 0.97 | 0.57 | 0.53 | 2.66E-06 | 1.61 | 1.31 to 2 |
| rs58923164 | 21 | 44 158 451 | <i>PDE9A</i> | T/G | 0.04 | 1 | 1 | 2.68E-06 | 1.34 | 1.17 to 1.53 |
| rs13433914 | 3 | 159 902 148 | <i>IL12A-AS1</i> | C/G | 0.22 | 0.71 | 0.63 | 2.74E-06 | 1.17 | 1.09 to 1.25 |
| rs2371887 | 2 | 214 085 179 | NA | G/A | 0.43 | 0.33 | 0.97 | 2.79E-06 | 1.15 | 1.08 to 1.21 |
| rs1717501 | 10 | 14 354 673 | <i>FRMD4A</i> | C/A | 0.12 | 0.57 | 0.55 | 3.07E-06 | 1.23 | 1.13 to 1.34 |
| rs138815617 | 17 | 19 445 425 | <i>SLC47A1</i> | A/G | 0.01 | 0.6 | 1 | 3.28E-06 | 1.54 | 1.22 to 1.94 |
| rs12430303 | 13 | 43 032 027 | <i>TNFSF11</i> | C/T | 0.45 | 0.4 | 0.57 | 3.61E-06 | 1.13 | 1.07 to 1.2 |
| rs186715000 | 4 | 1 589 324 | NA | G/A | 0.01 | 1 | 0.27 | 3.72E-06 | 1.52 | 1.24 to 1.87 |
| rs7043505 | 9 | 117 628 528 | <i>TNFSF8</i> | A/G | 0.55 | 0.47 | 0.25 | 3.74E-06 | 1.15 | 1.08 to 1.21 |
| rs72657048 | 1 | 25 289 734 | <i>RUNX3</i> | G/C | 0.5 | 0.65 | 0.77 | 3.90E-06 | 1.14 | 1.08 to 1.21 |
| rs7647909 | 3 | 71 200 157 | <i>FOXP1</i> | G/T | 0.24 | 0.13 | 0.6 | 4.56E-06 | 1.16 | 1.09 to 1.23 |
| rs11692867 | 2 | 100 759 477 | <i>AFF3</i> | G/A | 0.64 | 0.53 | 0.6 | 4.57E-06 | 1.13 | 1.07 to 1.2 |
| rs80136777 | 3 | 45 931 005 | <i>CCR9</i> | T/A | 0.88 | 0.57 | 0.2 | 4.68E-06 | 1.2 | 1.1 to 1.32 |
| rs139529714 | 4 | 169 369 671 | <i>DDX60L</i> | C/T | 0.01 | 1 | 0.27 | 4.78E-06 | 1.52 | 1.24 to 1.87 |
| rs521786 | 11 | 129 607 371 | NA | C/A | 0.11 | 0.65 | 0.11 | 4.94E-06 | 1.19 | 1.09 to 1.3 |
| rs661171 | 11 | 110 016 519 | <i>ZC3H12C</i> | G/T | 0.72 | 0.82 | 0 | 4.95E-06 | 1.16 | 1.09 to 1.24 |
| rs6506561 | 18 | 8 233 559 | <i>PTPRM</i> | T/C | 0.55 | 0.86 | 0.1 | 5.00E-06 | 1.13 | 1.07 to 1.19 |

Genome-wide significant loci for juvenile idiopathic arthritis are highlighted in bold.

bp, base pair; Chr., chromosome; HLA, human leucocyte antigen; HWE, Hardy-Weinberg equilibrium; RAF, risk allele frequency; SNP, single nucleotide polymorphism.

10^{-6}), BATF (p value = 1.51×10^{-4}) and FOXA2 (p value = 9.06×10^{-4}). Enrichment of JIA susceptibility SNPs was also identified to cell-type specific enhancers in three broad tissue types: blood, thymus, and gastrointestinal tract (online supplemental table 5, online supplemental figure 3). Specially, JIA SNPs showed over-representation of enhancers in different subsets of T cells, pointing to primary effector/memory T cells, primary T helper memory cells, primary T helper 17, primary natural killer and primary T regulatory cells as key players for JIA pathogenesis. Enrichment in active promoters was observed in a wider range of tissue/cell types, with GM12878 lymphoblastoid B cells showing

the strongest over-representation (p value = 1.06×10^{-3}) (online supplemental table 6, online supplemental figure 4).

Given the expected correlation between the analysed annotations, we then proceeded to perform a stepwise selection process to select a subset of non-redundant annotations. A combined model derived from all categories of annotations consisted of binding sites for RELA and EBF1, and enhancers in primary T helper memory cells and the T cell leukaemia cell line DND-41. The maximum likelihood of this cross-category model exceeded that from any of the single-annotation models thus identifying the most statistically relevant regulatory elements

Table 2 SNP showing genome-wide significant or suggestive associations with juvenile idiopathic arthritis in the meta-analysis

| SNP | Chr. | Position (bp) | Notable genes | Risk/non-risk allele | UK GWAS P value | USA GWAS P value | META P value | META OR | META 95% CI | Q statistic | Q P value | I ² |
|------------|------|---------------|---------------|----------------------|-----------------|------------------|--------------|---------|-------------|-------------|-----------|----------------|
| rs2614258 | 6 | 135 677 202 | AH11 | A/G | 9.17E-08 | 6.50E-06 | 9.47E-12 | 1.17 | 1.12–1.22 | 0.18 | 0.67 | 0 |
| rs79815064 | 3 | 46 277 577 | CCR3 | A/G | 7.61E-08 | 8.43E-05 | 3.31E-11 | 1.25 | 1.17–1.34 | 0.87 | 0.35 | 0 |
| rs12430303 | 13 | 43 032 027 | TNFSF11 | C/T | 3.61E-06 | 9.23E-04 | 1.88E-09 | 1.14 | 1.09–1.19 | 0.56 | 0.45 | 0 |
| rs7647909 | 3 | 71 200 157 | FOXP1 | G/T | 4.56E-06 | 5.27E-05 | 2.02E-09 | 1.17 | 1.11–1.23 | 0 | 0.96 | 0 |
| rs7043505 | 9 | 117 628 528 | TNFSF8 | A/G | 3.74E-06 | 0.008333 | 8.27E-08 | 1.12 | 1.07–1.17 | 1.09 | 0.3 | 0.08 |
| rs11692867 | 2 | 100 759 477 | AFF3 | G/A | 4.57E-06 | 0.004152 | 9.26E-08 | 1.13 | 1.08–1.19 | 0.59 | 0.44 | 0 |
| rs72657048 | 1 | 25 289 734 | RUNX3 | G/C | 3.90E-06 | 0.008138 | 3.51E-07 | 1.13 | 1.08–1.18 | 0.69 | 0.41 | 0 |

bp, base pair; Chr., chromosome; GWAS, genome-wide association study; SNP, single nucleotide polymorphism.

(figure 2). No annotations in the final model were excluded with cross-validation.

Prioritising potential causal SNPs

Using our high-density SNP panel, we aimed to identify the putative causal SNPs driving the association signals. For this purpose, we applied a Bayesian fine-mapping approach¹⁷ to define the PIP of each variant being causal given all other variants in the region. We fine-mapped each of the five newly discovered loci and 12 previously reported non-MHC susceptibility loci (p value $<5 \times 10^{-6}$ in the present study) to identify 95% credible SNP sets. There was no evidence to support multiple distinct association signals at any locus. For 5 (29%) and 10 (59%) of the 17 loci, fine-mapping resolved the association signal to 95% credible sets of ≤ 10 and ≤ 30 causal variants, respectively (online supplemental tables 7 and 8). Moreover, we identified five SNPs with PIPs of at least 0.5 for the following loci: RSBN1-PTPN22 (1p13.2; rs6679677), FOXP1 (3p13; rs7647909), CCR3 (3p21.31; rs79815064), ANKRD55 (5q11.2; rs7731626) and TYK2 (19p13.2; rs34536443) (online supplemental table 7). Interestingly, the method was able to identify rs34536443, a well-characterised non-synonymous variant in autoimmunity,²⁵ as the likely causal variant for TYK2 locus with a PIP of 80%.

Prioritising target genes

The identification of the target genes of the disease-associated variants is a crucial step towards describing the biological impact of a statistical association. To address this question, we first used eQTL data derived from 15 disease relevant immune cell types to correlate the identified credible SNPs with genes in each locus. The credible SNP sets captured the lead eQTL SNP for 15 genes (eGenes) at nine loci (figure 3 and online supplemental table 9). These observations were supported by statistical colocalisation (online supplemental table 10). Subsequently, we complemented the identification of the putative target genes of JIA SNPs by analysing high-resolution maps of enhancer-promoter interactions in human B and T cells. We observed HiChIP interactions for the promoters of 6 out of the 15 JIA eGenes: IL2RA, CLN3, ATP2A1, IL6ST, CCDC101 (SGF29) and ERAP2 (online supplemental table 11). In addition, SULT1A2, SULT1A1, ACTA2, FAS and AH11 promoters were located within 1 kb windows of JIA credible SNPs that overlapped an H3K27ac peak as identified from HiChIP data. We also observed promoter interactions for JIA credible SNPs and the promoters of IL2RA, CLN3, IL6ST, CCDC101 and ERAP2 through chromatin interaction maps obtained by capture Hi-C experiments (online supplemental table 12).

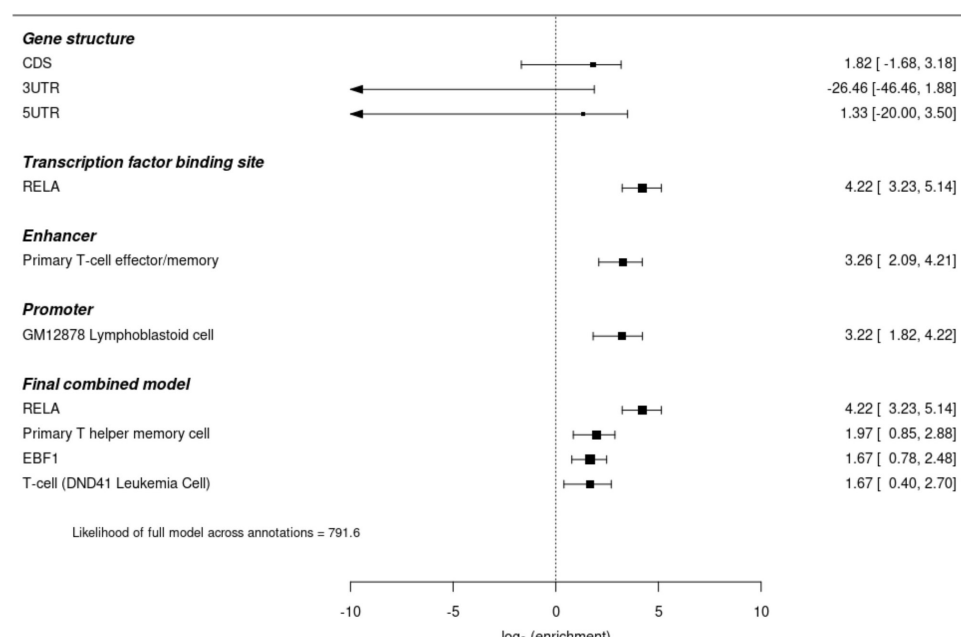


Figure 2 Functional enrichment analysis for JIA associations. Forest plot representing enrichment analysis results across four annotation categories based on experimental functional genomic data, and the final statistical annotation model. JIA, juvenile idiopathic arthritis.

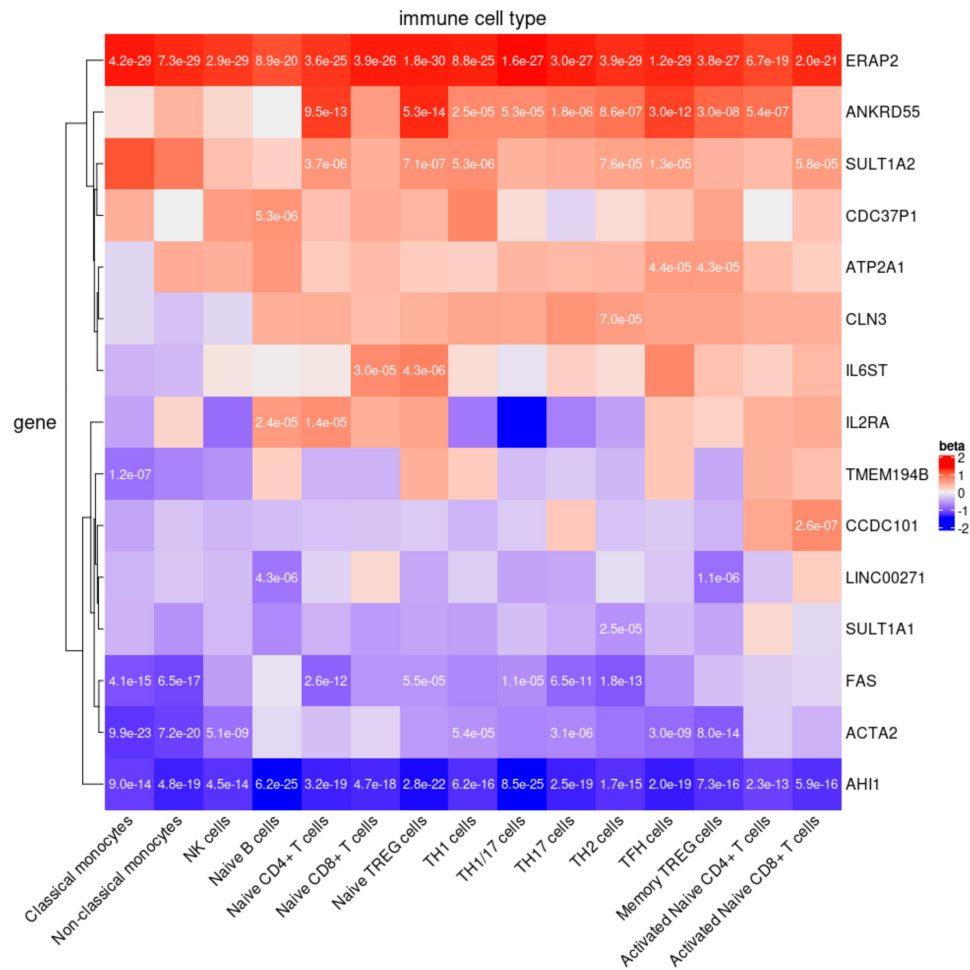


Figure 3 eQTL analysis. Significant eQTL from 15 disease relevant cell types of the DICE database including three innate immune cell types (classical monocytes, non-classical monocytes and natural killer cells), four adaptive immune cell types that have not encountered cognate antigen in the periphery (naive B cells, naive CD4⁺ T cells, naive CD8⁺ T cells and naive regulatory T cells (Treg)), six CD4⁺ memory or more differentiated T cell subsets (Th1, Th1/17, Th17, Th2, follicular helper T cell (Tfh) and memory Treg), and two activated cell types (naive CD4⁺ and CD8⁺ T cells that were stimulated ex vivo). The p value for significant correlations are reported in each cell for credible SNPs that capture the most significant eQTL. Beta coefficients to illustrate direction and magnitude as determined by risk allele. eQTL, expression quantitative trait locus; SNPs, single nucleotide polymorphisms.

Interestingly, our analysis allowed us to refine the target gene of the association signal at 5q11.2 to *IL6ST*, since the credible SNP (rs7731626) showed chromatin contacts to the promoter of this gene but we did not observe interactions to the classically reported gene *ANKRD55* (figure 4). This exemplifies the potential of integrative analyses in deciphering the plausible mechanistic effect of association signals.

In total, we found 11 JIA targets genes showing both significant eQTL and H3K27ac HiChIP evidence.

DISCUSSION

We used a Bayesian model selection approach to demonstrate extensive sharing of JIA susceptibility loci across the ILAR subtypes and subsequent joint analysis of subtypes led to the identification of five novel risk loci, bringing the total of genome-wide significant regions for JIA to 22. We were able to prioritise causal genes at six loci integrating Bayesian fine-mapped credible SNPs, transcriptomics and chromatin interaction maps derived from disease-relevant cells.

A key challenge for studies investigating JIA susceptibility is how to account for the clinical heterogeneity across the ILAR clinical subtypes. Previous studies have focussed on the more

frequent ILAR subtypes in an attempt to mitigate the loss of power due a non-specific phenotype definition.²⁶ However, in the present study this would have resulted in the exclusion of 30% of the available cases. Guided by the Bayesian model selection, we chose to perform a combined analysis across all ILAR subtypes, which we show maximises power to detect novel loci. However, it is important to recognise that this approach will only increase power to detect loci that underlie biological pathways shared by multiple ILAR subtypes and does not exclude the existence of subtype specific risk factors, which are known to exist.^{7,9,27}

Enrichment of JIA susceptibility loci in functional annotations highlighted that most association signals affect disease risk through regulatory effects on gene expression and in a cell-type specific manner. Our analysis pointed to the TFBS of RELA and EBF1 as two main non-redundant regulatory elements suggesting a crucial contribution of them in JIA risk. Interestingly, RELA and EBF1 are known to regulate Treg-induced tolerance²⁸ and B cell specification and commitment,²⁹ respectively.

Identifying target genes of the association signals is a crucial step to translate statistical findings to biological meaning and, in turn, for the development of new therapeutic strategies. Applying

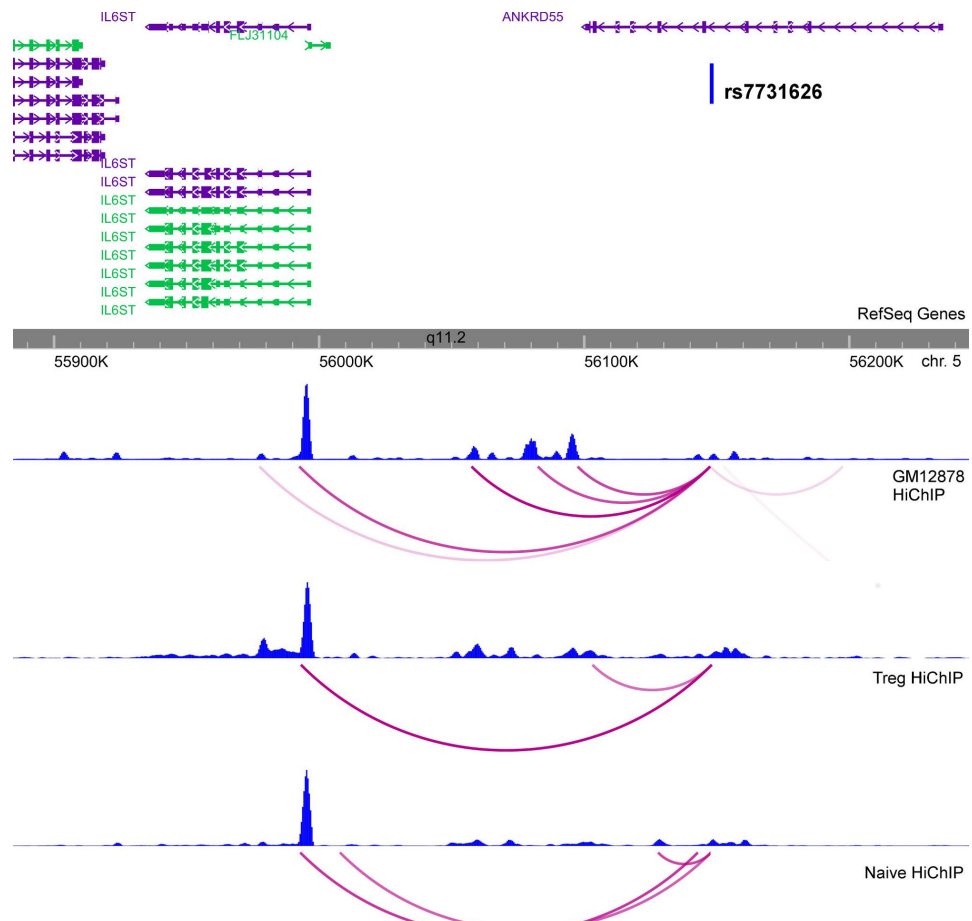


Figure 4 Chromatin interaction analysis at the *ANKRD55* locus. H3K27ac HiChIP signal at 5q11.2 showing enhancer-promoter chromatin interaction of rs7731626 to *IL6ST*. Blue graphs represent overlap with H3K27ac ChIP-seq peaks.

an integrative approach, we provide robust evidence to nominate target genes at the novel locus at 16p11.2. This is a known susceptibility locus for multiple chronic inflammatory diseases and includes attractive biological candidate genes such as *IL27*. However, complementary evidence from eQTL and chromatin data implicates the genes *CLN3* and *SULT1A2*. *CLN3* encodes a protein that is involved in lysosomal function suggesting a role for lysosome-mediated degradative pathways via autophagy and phagocytosis. Interestingly, Peeters *et al* reported that synovial fluid T cells derived from JIA patients showed enhanced autophagy.³⁰ *SULT1A2* encodes a catalytic enzyme that sulfonates different molecular components like thyroid hormones. Therefore, this target gene may establish a link for the comorbidity observed between rheumatic conditions and thyroid disorders. A second example of successful refinement is the association signal at 5q11.2 to *IL6ST*, instead of the classically reported gene *ANKRD55*.⁶ We found that the *ANKRD55* intronic SNP, rs7731626, interacts with the promoter of *IL6ST*, and that its risk allele increases the expression of the gene. *IL6ST* is the interleukin 6 (IL-6) signal transducer and is the drug target of satralizumab, a biological drug that is currently in Phase III of a clinical trial for neuromyelitis optica, a rare autoimmune disease of the nervous system.³¹ Considering that other biological drugs targeting the IL-6 pathway, such as tocilizumab, are currently in use for the treatment of JIA, our findings provide genetic support for the study of satralizumab as a new therapeutic target for JIA.

In conclusion, our results highlight the utility of joint analysis considering all JIA subtypes to maximise discovery, shifting the

classical paradigm on which previous JIA genetic studies were based, and illustrate the potential of integrative approaches to gain further insights into the genetic susceptibility of the disease, which may in turn inform future therapeutic drug targets and pathways.

Author affiliations

¹Centre for Genetics and Genomics Versus Arthritis, Centre for Musculoskeletal Research, Manchester Academic Health Science Centre, The University of Manchester, Manchester, UK

²Center for Public Health Genomics and Department of Biostatistical Sciences, Wake Forest University School of Medicine, Winston-Salem, North Carolina, USA

³Division of Rheumatology, Cincinnati Children's Hospital Medical Center and University of Cincinnati, Cincinnati, Ohio, USA

⁴The Lydia Becker Institute of Immunology and Inflammation, Faculty of Biology, Medicine and Health, The University of Manchester, Manchester, UK

⁵Department of Pediatrics and Human Genetics, Emory University, and Children's Healthcare of Atlanta, Atlanta, Georgia, USA

⁶National Institute of Health Research Manchester Biomedical Research Centre, Manchester Academic Health Science Centre, Manchester University NHS Foundation Trust, Manchester, UK

Acknowledgements This study acknowledges the use of the following UK JIA cohort collections: British Society of Paediatric and Adolescent Rheumatology (BSPAR) study group, Childhood Arthritis Prospective Study (CAPS) (funded by Versus Arthritis, grant reference number 20542), Childhood Arthritis Response to Medication Study (CHARMS) (funded by Sparks UK, reference 08ICH09 and the Medical Research Council, reference MR/M004600/1), United Kingdom Juvenile Idiopathic Arthritis Genetics Consortium (UKJAGC). We thank Versus Arthritis for their support. This research was funded by the NIHR Manchester Biomedical Research Centre and supported by the Manchester Academic Health Sciences Centre (MAHSC). The views expressed are those of the author(s) and not necessarily those of the NHS, the NIHR or the Department of Health. We would like to acknowledge

Paediatric rheumatology

the assistance given by IT Services and the use of the Computational Shared Facility at The University of Manchester. Understanding Society: The UK Household Longitudinal Study is led by the Institute for Social and Economic Research at the University of Essex and funded by the Economic and Social Research Council. The survey was conducted by NatCen and the genome-wide scan data were analysed and deposited by the Wellcome Trust Sanger Institute.

Contributors JB and WT contributed to the conception and study design. JB, EL-I, SS, AY, MCM, MS, SP, CDL and SDT contributed to Data collection and/or QC and imputation. EL-I, JB, APM, CS, PM and VPG contributed to data analysis. JB, EL-I and WT were involved in drafting the manuscript. All co-authors made substantial contributions to data acquisition, data interpretation and revised the work critically for important intellectual content.

Funding Versus Arthritis, grant (20542); Sparks UK, (08ICH09); the Medical Research Council, grant reference (MR/M004600/1). Genotyping of the UK JIA case samples was supported by the Versus Arthritis grants (20385 and 21754). This research was funded by the NIHR Manchester Biomedical Research Centre and supported by the MAHSC.

Competing interests None declared.

Patient consent for publication Not required.

Ethics approval JIA participants were recruited with ethical approval and provided informed consent, including from the North West Multi-centre for Research Ethics Committee (MREC: 02/8/104 and MREC: 99/8/84), West Midlands Multi-centre Research Ethics Committee (MREC: 02/7/106), North West Research Ethics Committee (REC: 09/H1008/137) and the NHS Research Ethics Committee (REC: 05/Q0508/95).

Provenance and peer review Not commissioned; externally peer reviewed.

Data availability statement Data are available in a public, open access repository. All data relevant to the study are included in the article or uploaded as supplementary information. Summary statistics of the GWAS analysed in the current study will be available through the NHGRI-EBI GWAS Catalog (<https://www.ebi.ac.uk/gwas/downloads/summary-statistics>) (Study Accession Code GCST90010715). Healthy controls data was obtained from the UK Household Longitudinal Study (<https://www.understandingsociety.ac.uk/>). Information on how to access the data can be found on the Understanding Society website <https://www.understandingsociety.ac.uk/>.

Supplemental material This content has been supplied by the author(s). It has not been vetted by BMJ Publishing Group Limited (BMJ) and may not have been peer-reviewed. Any opinions or recommendations discussed are solely those of the author(s) and are not endorsed by BMJ. BMJ disclaims all liability and responsibility arising from any reliance placed on the content. Where the content includes any translated material, BMJ does not warrant the accuracy and reliability of the translations (including but not limited to local regulations, clinical guidelines, terminology, drug names and drug dosages), and is not responsible for any error and/or omissions arising from translation and adaptation or otherwise.

Open access This is an open access article distributed in accordance with the Creative Commons Attribution 4.0 Unported (CC BY 4.0) license, which permits others to copy, redistribute, remix, transform and build upon this work for any purpose, provided the original work is properly cited, a link to the licence is given, and indication of whether changes were made. See: <https://creativecommons.org/licenses/by/4.0/>.

ORCID iDs

Elena López-Isac <http://orcid.org/0000-0001-8806-5148>
 Samantha L Smith <http://orcid.org/0000-0002-4108-8497>
 Annie Yarwood <http://orcid.org/0000-0001-5026-9815>
 Paul Martin <http://orcid.org/0000-0002-1016-6851>
 Sampath Prahalad <http://orcid.org/0000-0003-3489-1756>
 John Bowes <http://orcid.org/0000-0003-4659-031X>

REFERENCES

- Okada Y, Wu D, Trynka G, et al. Genetics of rheumatoid arthritis contributes to biology and drug discovery. *Nature* 2014;506:376–81.
- Nelson MR, Tipney H, Painter JL, et al. The support of human genetic evidence for Approved drug indications. *Nat Genet* 2015;47:856–60.
- Prakken B, Albani S, Martini A. Juvenile idiopathic arthritis. *Lancet* 2011;377:2138–49.
- Petty RE, Southwood TR, Manners P, et al. International League of associations for rheumatology classification of juvenile idiopathic arthritis: second revision, Edmonton, 2001. *J Rheumatol* 2004;31:390–2.
- Thompson SD, Sudman M, Ramos PS, et al. The susceptibility loci juvenile idiopathic arthritis shares with other autoimmune diseases extend to PTPN2, COG6, and ANGPT1. *Arthritis Rheum* 2010;62:3265–76.
- Hinks A, Cobb J, Marion MC, et al. Dense genotyping of immune-related disease regions identifies 14 new susceptibility loci for juvenile idiopathic arthritis. *Nat Genet* 2013;45:664–9.
- Hinks A, Bowes J, Cobb J, et al. Fine-Mapping the MHC locus in juvenile idiopathic arthritis (JIA) reveals genetic heterogeneity corresponding to distinct adult inflammatory arthritic diseases. *Ann Rheum Dis* 2017;76:765–72.
- McIntosh LA, Marion MC, Sudman M, et al. Genome-Wide association meta-analysis reveals novel juvenile idiopathic arthritis susceptibility loci. *Arthritis Rheumatol* 2017;69:2222–32.
- Ombrello MJ, Arthur VL, Remmers EF, et al. Genetic architecture distinguishes systemic juvenile idiopathic arthritis from other forms of juvenile idiopathic arthritis: clinical and therapeutic implications. *Ann Rheum Dis* 2017;76:906–13.
- Ombrello MJ, Remmers EF, Tachmazidou I, et al. HLA-DRB1*11 and variants of the MHC class II locus are strong risk factors for systemic juvenile idiopathic arthritis. *Proc Natl Acad Sci U S A* 2015;112:15970–5.
- Jostins L, McVean G, Trinculo: Bayesian and frequentist multinomial logistic regression for genome-wide association studies of multi-category phenotypes. *Bioinformatics* 2016;32:1898–900.
- Abraham G, Qiu Y, Inouye M. FlashPCA2: principal component analysis of Biobank-scale genotype datasets. *Bioinformatics* 2017;33:2776–8.
- Bellenguez C, Strange A, Freeman C, et al. A robust clustering algorithm for identifying problematic samples in genome-wide association studies. *Bioinformatics* 2012;28:134–5.
- Delaneau O, Zagury J-F, Marchini J. Improved whole-chromosome phasing for disease and population genetic studies. *Nat Methods* 2013;10:5–6.
- Das S, Forer L, Schönherr S, et al. Next-Generation genotype imputation service and methods. *Nat Genet* 2016;48:1284–7.
- Mägi R, Morris AP. GWAMA: software for genome-wide association meta-analysis. *BMC Bioinformatics* 2010;11:288.
- Benner C, Spencer CCA, Havulinna AS, et al. FINEMAP: efficient variable selection using summary data from genome-wide association studies. *Bioinformatics* 2016;32:1493–501.
- Harrow J, Frankish A, Gonzalez JM, et al. GENCODE: the reference human genome annotation for the encode project. *Genome Res* 2012;22:1760–74.
- ENCODE Project Consortium. An integrated encyclopedia of DNA elements in the human genome. *Nature* 2012;489:57–74.
- Chadwick LH. The NIH roadmap epigenomics program data resource. *Epigenomics* 2012;4:317–24.
- Pickrell JK. Joint analysis of functional genomic data and genome-wide association studies of 18 human traits. *Am J Hum Genet* 2014;94:559–73.
- Schmidel BJ, Singh D, Madrigal A, et al. Impact of genetic polymorphisms on human immune cell gene expression. *Cell* 2018;175:1701–15, e16.
- Mumbach MR, Satpathy AT, Boyle EA, et al. Enhancer connectome in primary human cells identifies target genes of disease-associated DNA elements. *Nat Genet* 2017;49:1602–12.
- Martin P, McGovern A, Orozco G, et al. Capture Hi-C reveals novel candidate genes and complex long-range interactions with related autoimmune risk loci. *Nat Commun* 2015;6:10069.
- Dendrou CA, Cortes A, Shipman L, et al. Resolving Tyk2 locus genotype-to-phenotype differences in autoimmunity. *Sci Transl Med* 2016;8:363ra149.
- Sham PC, Purcell SM. Statistical power and significance testing in large-scale genetic studies. *Nat Rev Genet* 2014;15:335–46.
- Hinks A, Marion MC, Cobb J, et al. Brief report: the genetic profile of rheumatoid factor-positive polyarticular juvenile idiopathic arthritis resembles that of adult rheumatoid arthritis. *Arthritis Rheumatol* 2018;70:957–62.
- Messina N, Fulford T, O'Reilly L, et al. The NF-κB transcription factor RelA is required for the tolerogenic function of Foxp3(+) regulatory T cells. *J Autoimmun* 2016;70:52–62.
- Nechamitzky R, Akbas D, Scherer S, et al. Transcription factor EBF1 is essential for the maintenance of B cell identity and prevention of alternative fates in committed cells. *Nat Immunol* 2013;14:867–75.
- Peeters JGC, de Graeff N, Lotz M, et al. Increased autophagy contributes to the inflammatory phenotype of juvenile idiopathic arthritis synovial fluid T cells. *Rheumatology* 2017;56:1694–9.
- Carvalho-Silva D, Pierleoni A, Pignatelli M, et al. Open targets platform: new developments and updates two years on. *Nucleic Acids Res* 2019;47:D1056–65.

1

SUPPLEMENTARY MATERIAL**2 TABLE OF CONTENTS**

| | | |
|----|---|----|
| 3 | 1.- Online Supplementary Methods | 2 |
| 4 | 1.1 Study cohort | 2 |
| 5 | 1.2 Genotyping and quality control | 2 |
| 6 | 1.3 Imputation | 3 |
| 7 | 1.4 Association testing and meta-analysis | 4 |
| 8 | 1.5 Heritability estimation | 4 |
| 9 | 1.6 Clinical subtype specificity | 4 |
| 10 | 1.7 Statistical fine-mapping of JIA-associated loci | 5 |
| 11 | 1.8 Functional annotation enrichment analysis | 5 |
| 12 | 1.9 Gene prioritisation with eQTL | 6 |
| 13 | 1.10 Chromatin interaction analysis in human B and T cell types | 6 |
| 14 | 2.- Supplementary Figure Legends | 8 |
| 15 | 3.- Supplementary Figures | 9 |
| 16 | 4.- Supplementary References..... | 13 |
| 17 | | |

18 **1. ONLINE SUPPLEMENTARY METHODS**

19 **1.1 Study cohort**

20 A total of 4,520 UK juvenile idiopathic arthritis (JIA) samples were recruited from
21 multiple sources: the British Society for Paediatric and Adolescent Rheumatology (BSPAR)
22 National Repository of JIA, the Childhood Arthritis Prospective Study (CAPS), the
23 Childhood Arthritis Response to Medication Study (CHARMS), the UK JIA Genetics
24 Consortium (UKJIAGC), The Biologics for Children with Rheumatic Diseases (BCRD)
25 study, and the British Society for Paediatric and Adolescent Rheumatology Etanercept Cohort
26 Study (BSPAR-ETN), a group of UK cases with long-standing JIA as described
27 previously[1]. JIA participants were recruited with ethical approval and provided informed
28 consent, including from the North West Multi-centre for Research Ethics Committee
29 (MREC:02/8/104 and MREC:99/8/84), West Midlands Multi-centre Research Ethics
30 Committee (MREC:02/7/106), North West Research Ethics Committee (REC:09/H1008/137)
31 and the NHS Research Ethics Committee (REC:05/Q0508/95). JIA cases were classified
32 according to the International League of Associations for Rheumatology (ILAR) criteria[2]
33 (Supplementary Table 1). Healthy controls data on 9,965 individuals was obtained from the
34 UK Household Longitudinal Study (<https://www.understandingsociety.ac.uk/>) accessed via
35 the European Genome-phenome Archive.

36 **1.2 Genotyping and quality control**

37 JIA DNA samples were genotyped on the Illumina Infinium CoreExome and Infinium
38 OnmiExpress genotyping arrays in accordance to the manufacturer's instructions. Genotype
39 calling was performed by the GenCall algorithm in the GenomeStudio Data Analysis software
40 platform (Genotyping Module v1.8.4). Preliminary genotype clustering was performed using
41 the default Illumina cluster file to identify poor quality samples (call rate < 0.90). Following
42 exclusion of low-quality samples, automated reclustering was performed to calibrate genotype

43 clusters based on the study samples. Sample-level quality control (QC) was performed based
44 on the following exclusion criteria: final call rate < 0.98, outlier based on autosomal
45 heterozygosity (2 standard deviations from the mean) and discrepancy between genetically
46 inferred sex and database records. Single-nucleotide polymorphisms (SNPs) were excluded if
47 they were non-autosomal, had a call rate < 0.98 or a minor allele frequency (MAF) < 0.01.
48 Healthy controls were genotyped at the Wellcome Trust Sanger Institute using the Illumina
49 Infinium CoreExome genotyping array. Sample and SNP QC was consistent with that
50 described above for JIA case samples.

51 The two datasets were combined retaining the intersection of SNPs. Identity-by-
52 descent was used to identify related individuals (kinship coefficient > 0.0884) across all study
53 samples performed with the KING software package (version 1.9)[3]. For each related pair,
54 the sample with the highest call rate was preferentially retained. Individuals were excluded if
55 they were identified as outliers based on ancestry using principal component analysis (PCA)
56 performed with the flashpca software package (version 2.0) where outliers were identified
57 using aberrant R library (version 1.0)[4,5].

58 The total number of individuals that remained in the final QC-filtered dataset was
59 12,501 (3,305 cases and 9,196 healthy controls).

60 1.3 Imputation

61 QC-filtered GWAS dataset was subjected to whole-genome genotype imputation.
62 Prior to imputation, SNPs with ambiguous alleles (C/G and A/T) were excluded and
63 remaining SNPs were aligned to the Haplotype Reference Consortium (HRC) panel (version
64 1.1) using the HRC imputation preparation tool
65 (<https://www.well.ox.ac.uk/~wrayner/tools/>)[6]. Phasing and imputation were performed in
66 the Michigan Imputation server using SHAPEIT2[7] and Minimac3[8] respectively, and HRC

67 panel for reference. Following imputation, SNPs were excluded based on a MAF < 0.01 and
68 imputation quality (r^2) < 0.4.

69 **1.4 Association testing and meta-analysis**

70 Case-control association testing was performed by SNPTEST software package
71 (version 2.5.2) using the score method to account for imputation uncertainty. Three principal
72 components, calculated as described above following exclusion of outliers, were included as
73 covariates to account for any residual population sub-structure. Lambda genomic control
74 (λ_{GC}), corrected for sample size (λ_{1000}), was calculated to test for inflation of test statistics
75 attributable to population stratification not accounted for in the analysis. Any SNP with a p-
76 value $< 5 \times 10^{-6}$ was selected for validation in GWAS summary statistics from an independent
77 dataset of 2,751 JIA cases (oligoarticular arthritis (oligoJIA) and rheumatoid factor (RF)-
78 negative polyarthritis (RF-polyJIA)) and 15,886 controls of European Ancestry[9]. An
79 inverse variance weighted fixed effects meta-analysis was performed using the software
80 package GWAMA (version 2.2.2)[10]. The presence of heterogeneity of odds ratios (ORs)
81 across datasets was evaluated with the test statistics I^2 and Q.

82 **1.5 Heritability estimation**

83 SNP-based heritability estimates were calculated using GCTA based on imputed data
84 for all JIA cases[11]. Imputed SNPs were stratified into linkage disequilibrium (LD) score
85 bins and a genetic relationship matrix (GRM) was calculated separately for each bin followed
86 by restricted maximum likelihood (REML) analysis performed on the multiple GRMs.

87 **1.6 Clinical subtype specificity**

88 The specificity and sharing of JIA susceptibility SNPs across ILAR subtypes was
89 interrogated using Bayesian multinomial logistic regression assuming an additive model
90 implemented in the software package Trinculo (version 0.96) using default correlation priors
91 (0.04) for all index SNPs with p-value $< 5 \times 10^{-6}$ [12]. In addition, we have included previously

92 reported JIA susceptibility SNPs based on analysis of a combined oligoJIA and RF-polyJIA
93 cohort[13]. Trinculo identifies the best disease-specific model, the best sharing model, and
94 estimates the Bayes factor between them at each analysed locus. Model selection was based
95 on comparison of log-Bayes factors where a positive log-Bayes factor for specificity was
96 interpreted as evidence that a particular association is specific to an ILAR subtype and a
97 negative value indicative of sharing across multiple ILAR subtypes. The undifferentiated
98 subtype was not included in this analysis.

99 **1.7 Statistical fine-mapping of JIA-associated loci**

100 The boundaries of independently associated loci were defined by a genetic distance of
101 0.1 centimorgans (cM) upstream and downstream of each lead SNP using HapMap fine-scale
102 recombination rate estimates. Statistical fine-mapping of the association signal within each
103 locus was performed using the FINEMAP software package (version 1.3.1) using the shotgun
104 stochastic search function to identify independent effects using an LD panel of 4,000
105 randomly selected controls from the Understanding Society dataset[14]. The 95% credible
106 SNP sets for each locus were selected on the summation of the posterior inclusion
107 probabilities (PIPs) for the most likely causal SNPs. Any independent effects within each
108 locus identified by the stochastic search approach were verified by conditional and joint
109 analysis using GCTA-COJO with the same LD panel as FINEMAP (version 1.92.4)[15]. All
110 identified credible SNPs were annotated with gene location based on RefSeq transcript and
111 evidence for association with other diseases using data from the GWAS catalogue[16]. Non-
112 synonymous credible SNPs were annotated with the pre-calculated Combined Annotation
113 Dependent Depletion (CADD) raw score and scaled score from dbNSFP (version 3.3a)[17].
114 Annotation was performed with ANNOVAR (version 2019Oct24)[18].

115 **1.8 Functional annotation enrichment analysis**

116 Summary statistics from the association analysis of all ILAR subtypes were tested for
117 enrichment in four categories of annotations based on experimental functional genomic data
118 including gene structure (coding sequence (CDS), 3`UTR and 5`UTR) from the GENCODE
119 Project, binding sites for 165 transcription factors from the ENCODE Project, and enhancers
120 and active promoters for 98 cell types derived from the Roadmap Epigenomics Project[19–
121 21]. Enrichment of JIA associations were tested separately in each annotation using fgwas
122 (version 0.3.6)[22]. A joint model of independent enrichments was identified using a forward
123 selection approach of selecting the most significant annotation and sequentially adding
124 additional significant annotations and retaining those that significantly increase the likelihood
125 of the joint model using cross-validation with penalised likelihood to identify the model with
126 the highest cross-validation likelihood.

127 **1.9 Gene prioritisation with eQTL**

128 Expression quantitative trait locus (eQTL) data for 15 cell types was downloaded from
129 the DICE (Database of Immune Cell Expression, eQTLs and Epigenomics) project
130 website[23]. Cell types consisted of three innate immune cell types ($CD14^{high}$ $CD16^-$ classical
131 monocytes, $CD14^- CD16^+$ non-classical monocytes, $CD56^{dim}$ $CD16^+$ natural killer (NK) cells),
132 four adaptive immune cell types that have not encountered cognate antigen in the periphery
133 (naive B cells, naive $CD4^+$ T cells, naive $CD8^+$ T cells, and naive regulatory T cells [Treg]),
134 six $CD4^+$ memory or more differentiated T cell subsets (T_{H1} , $T_{H1/17}$, T_{H17} , T_{H2} , follicular
135 helper T cell [Tfh], and memory Treg [mTreg]), and two activated cell types (naive $CD4^+$ and
136 $CD8^+$ T cells that were stimulated *ex vivo*) (description from DICE website <https://dice-database.org/>). Correlation of susceptibility association signals and gene expression were
137 identified by selecting the top eQTL SNP for each gene in each eQTL dataset and retaining
138 those that were also present in the combined list of all FINEMAP credible SNPs for

140 associated loci. Colocalisation of the susceptibility association and eQTL signals was then
141 confirmed using the coloc R package using approximate Bayes factors[24].

142 **1.10 Chromatin interaction analysis in human B and T cell types**

143 Prioritisation of causal genes was further complemented by the interrogation of
144 chromatin interaction data for SNPs correlated with eQTL signals. H3K27ac HiChIP data in
145 GM12878, primary human naïve T cells ($CD4^+CD45RA^+CD25^-CD127^{high}$), regulatory T
146 (Treg) cells ($CD4^+CD25^+CD127^{low}$) and T_{H17} cells ($CD4^+CD45RA^-CD25^-$
147 $CD127^{high}CCR6^+CXCR5^-$) were interrogated to identify target genes of JIA-associated
148 regions[25]. In detail, sequencing data for the HiChIP libraries was filtered and the adapters
149 were removed using fastp v0.19.4[26]. Then we mapped the reads to the human reference
150 genome GRCh38 with Hi-C Pro v2.11.0 using default settings[27]. HiChIP-peaks v0.1.1 was
151 used with default settings and false discovery rate (FDR) < 0.01 to identify H3K27ac peaks
152 enriched regions[28]. Identification of significant chromatin loops was performed with
153 FitHiChIP using the following settings: Coverage normalization, stringent background with
154 merging enabled, peaks generated from HiChIP-peaks and 5kb bin size[29]. We explored
155 chromatin interaction profiles of the credible SNPs sets from each locus. To identify the
156 connectivity of credible SNPs to target genes, we subsetted the interactions to those linking a
157 transcription start site (TSS) and SNPs overlapping a H3K27ac HiChIP peak in a 5kb
158 resolution. We also nominated the genes for which the TSS was within 1kb of a credible SNP
159 overlapping an H3K27ac peak as identified from HiChIP data. In addition, we explored
160 chromatin interaction maps obtained by capture Hi-C experiments in GM12878 and Jurkat
161 cell types[30]. Credible SNPs were set as anchor points to identify physical interactions
162 between restriction fragments containing the variants and gene promoters using IRanges and
163 GenomicRanges R packages.

164

165

166 **2. SUPPLEMENTARY FIGURE LEGENDS**

167 **Supplementary Figure 1. Bayesian model selection analysis for ILAR subtype**
168 **specificity of JIA susceptibility SNPs.** Comparison of log Bayes factor for best
169 specific ILAR subtype model (x axis) and best shared model (y axis). Susceptibility
170 SNPs (represented by blue dots for loci from this study, red dots for previously
171 published SNPs based on oligoJIA and RF-polyJIA) above the grey line indicate
172 evidence for sharing of association across multiple ILAR subtypes.

173 **Supplementary Figure 2. Enrichment of JIA susceptibility SNPs in transcription**
174 **factor binding sites.** Annotations showing significant enrichment are displayed in
175 green.

176 **Supplementary Figure 3. Enrichment of JIA susceptibility SNPs in regulatory**
177 **regions of 98 cells.** Supplementary Table 5 provides the correspondence between cell
178 codes and cell types.

179 **Supplementary Figure 4. Enrichment of JIA susceptibility SNPs in active**
180 **promoters of 98 cells.** Supplementary Table 6 provides the correspondence between
181 cell codes and cell types.

182

183

184

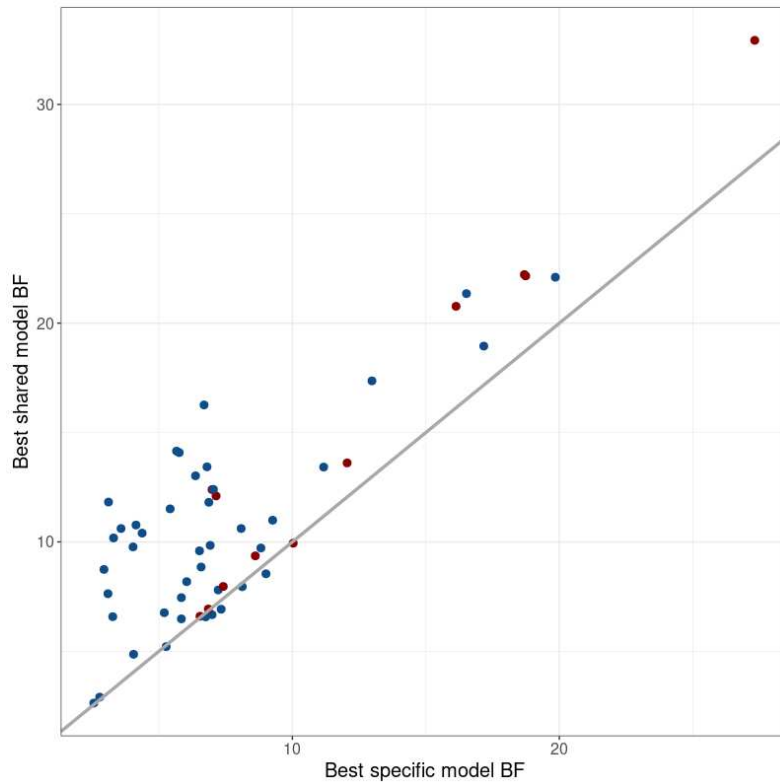
3. SUPPLEMENTARY FIGURES

185

Supplementary Figure 1

186

187

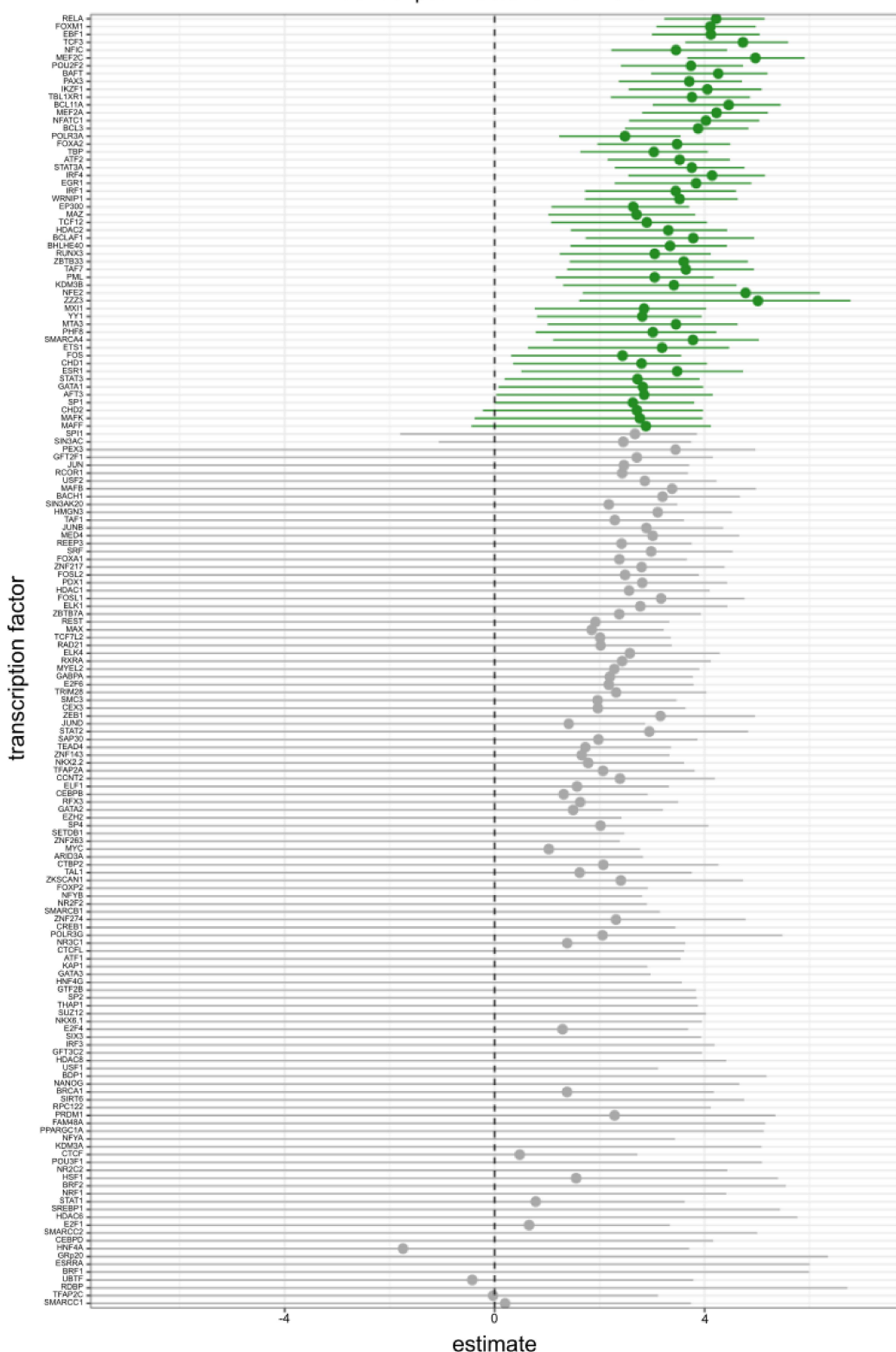


188

189

190 **Supplementary Figure 2**

transcription factor enrichment



191

192

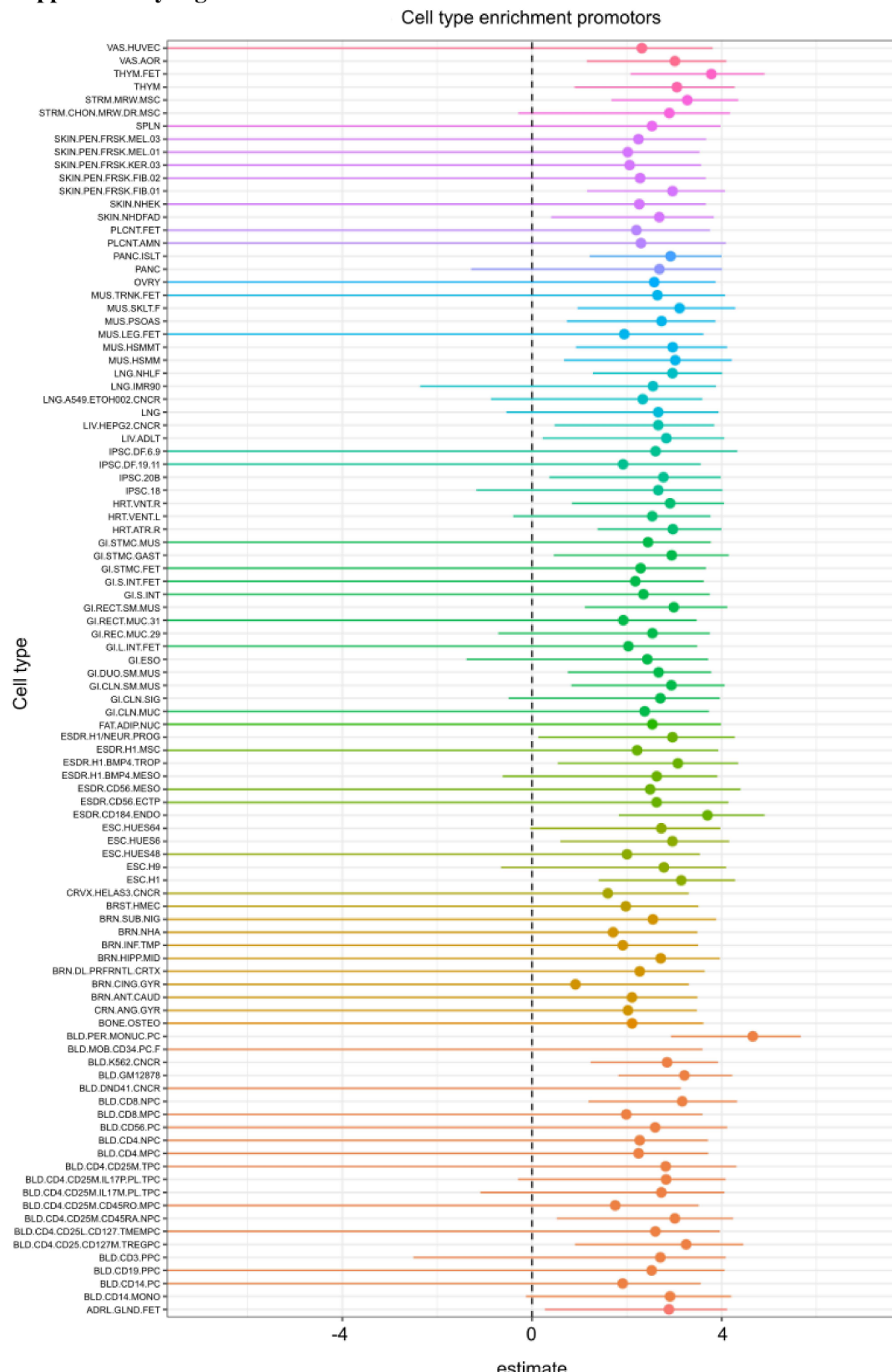
193 Supplementary Figure 3



194

12

195 Supplementary Figure 4



196

13

197 **4. SUPPLEMENTARY REFERENCES**

- 198 1 Packham JC, Hall MA. Long-term follow-up of 246 adults with juvenile idiopathic
199 arthritis: Functional outcome. *Rheumatology* 2002;**41**:1428–35.
200 doi:10.1093/rheumatology/41.12.1428
- 201 2 Petty RE, Southwood TR, Manners P, *et al.* International League of Associations for
202 Rheumatology classification of juvenile idiopathic arthritis: second revision,
203 Edmonton, 2001. *J Rheumatol* 2004;**31**:390–2.
- 204 3 Manichaikul A, Mychaleckyj JC, Rich SS, *et al.* Robust relationship inference in
205 genome-wide association studies. *Bioinformatics* 2010;**26**:2867–73.
206 doi:10.1093/bioinformatics/btq559
- 207 4 Abraham G, Qiu Y, Inouye M. FlashPCA2: principal component analysis of Biobank-
208 scale genotype datasets. *Bioinformatics* 2017;**33**:2776–8.
209 doi:10.1093/bioinformatics/btx299
- 210 5 Bellenguez C, Strange A, Freeman C, *et al.* A robust clustering algorithm for
211 identifying problematic samples in genome-wide association studies. *Bioinformatics*
212 2012;**28**:134–5. doi:10.1093/bioinformatics/btr599
- 213 6 McCarthy S, Das S, Kretzschmar W, *et al.* A reference panel of 64,976 haplotypes for
214 genotype imputation. *Nat Genet* 2016;**48**:1279–83. doi:10.1038/ng.3643
- 215 7 Delaneau O, Zagury JF, Marchini J. Improved whole-chromosome phasing for disease
216 and population genetic studies. *Nat Methods* 2013;**10**:5–6. doi:10.1038/nmeth.2307
- 217 8 Das S, Forer L, Schönherr S, *et al.* Next-generation genotype imputation service and
218 methods. *Nat Genet* 2016;**48**:1284–1287. doi:10.1038/ng.3656
- 219 9 McIntosh LA, Marion MC, Sudman M, *et al.* Genome-Wide Association Meta-
220 Analysis Reveals Novel Juvenile Idiopathic Arthritis Susceptibility Loci. *Arthritis*
221 *Rheumatol (Hoboken, NJ)* 2017;**69**:2222–32. doi:10.1002/art.40216
- 222 10 Magi R, Morris AP. GWAMA: software for genome-wide association meta-analysis.
223 *BMC Bioinformatics* 2010;**11**:288. doi:10.1186/1471-2105-11-288
- 224 11 Yang J, Manolio TA, Pasquale LR, *et al.* Genome partitioning of genetic variation for
225 complex traits using common SNPs. *Nat Genet* 2011;**43**:519–25. doi:10.1038/ng.823
- 226 12 Jostins L, McVean G. Trinculo: Bayesian and frequentist multinomial logistic
227 regression for genome-wide association studies of multi-category phenotypes.
228 *Bioinformatics* 2016;**32**:1898–900. doi:10.1093/bioinformatics/btw075
- 229 13 Hinks A, Cobb J, Marion MC, *et al.* Dense genotyping of immune-related disease

- 230 regions identifies 14 new susceptibility loci for juvenile idiopathic arthritis. *Nat Genet*
231 2013;45:664–9. doi:10.1038/ng.2614
- 232 14 Benner C, Spencer C, Havulinna AS, *et al.* FINEMAP: efficient variable selection
233 using summary data from genome-wide association studies. *Bioinformatics*
234 2016;32:1493–501. doi:10.1093/bioinformatics/btw018
- 235 15 Yang J, Ferreira T, Morris AP, *et al.* Conditional and joint multiple-SNP analysis of
236 GWAS summary statistics identifies additional variants influencing complex traits. *Nat*
237 *Genet* 2012;44:369–75, S1-3. doi:10.1038/ng.2213
- 238 16 MacArthur J, Bowler E, Cerezo M, *et al.* The new NHGRI-EBI Catalog of published
239 genome-wide association studies (GWAS Catalog). *Nucleic Acids Res* 2017;45:D896–
240 D901. doi:10.1093/nar/gkw1133
- 241 17 Liu X, Wu C, Li C, *et al.* dbNSFP v3.0: A One-Stop Database of Functional
242 Predictions and Annotations for Human Nonsynonymous and Splice-Site SNVs. *Hum*
243 *Mutat* 2016;37:235–41. doi:10.1002/humu.22932
- 244 18 Yang H, Wang K. Genomic variant annotation and prioritization with ANNOVAR and
245 wANNOVAR. *Nat Protoc* 2015;10:1556–66. doi:10.1038/nprot.2015.105
- 246 19 Harrow J, Frankish A, Gonzalez JM, *et al.* GENCODE: the reference human genome
247 annotation for The ENCODE Project. *Genome Res* 2012;22:1760–74.
248 doi:10.1101/gr.135350.111
- 249 20 ENCODE Project Consortium I, Kundaje A, Aldred SF, *et al.* An integrated
250 encyclopedia of DNA elements in the human genome. *Nature* 2012;489:57–74.
251 doi:10.1038/nature11247
- 252 21 Chadwick LH. The NIH Roadmap Epigenomics Program data resource. *Epigenomics*
253 2012;4:317–24. doi:10.2217/epi.12.18
- 254 22 Pickrell JK. Joint analysis of functional genomic data and genome-wide association
255 studies of 18 human traits. *Am J Hum Genet* 2014;94:559–73.
256 doi:10.1016/j.ajhg.2014.03.004
- 257 23 Schmiedel BJ, Singh D, Madrigal A, *et al.* Impact of Genetic Polymorphisms on
258 Human Immune Cell Gene Expression. *Cell* 2018;175:1701–1715.e16.
259 doi:10.1016/j.cell.2018.10.022
- 260 24 Giambartolomei C, Vukcevic D, Schadt EE, *et al.* Bayesian Test for Colocalisation
261 between Pairs of Genetic Association Studies Using Summary Statistics. *PLoS Genet*
262 2014;10:e1004383. doi:10.1371/journal.pgen.1004383
- 263 25 Mumbach MR, Satpathy AT, Boyle EA, *et al.* Enhancer connectome in primary human

- 264 cells identifies target genes of disease-associated DNA elements. *Nat Genet*
265 2017;**49**:1602–12. doi:10.1038/ng.3963
- 266 26 Chen S, Zhou Y, Chen Y, *et al.* fastp: an ultra-fast all-in-one FASTQ preprocessor.
267 *Bioinformatics* 2018;**34**:i884–90. doi:10.1093/bioinformatics/bty560
- 268 27 Servant N, Varoquaux N, Lajoie BR, *et al.* HiC-Pro: an optimized and flexible pipeline
269 for Hi-C data processing. *Genome Biol* 2015;**16**:259. doi:10.1186/s13059-015-0831-x
- 270 28 Shi C, Rattray M, Orozco G. HiChIP-Peaks: A HiChIP peak calling algorithm. *bioRxiv*
271 Published Online First: 2019. doi:10.1101/682781
- 272 29 Bhattacharyya S, Chandra V, Vijayanand P, *et al.* Identification of significant
273 chromatin contacts from HiChIP data by FitHiChIP. *Nat Commun* 2019;**10**:4221.
274 doi:10.1038/s41467-019-11950-y
- 275 30 Martin P, McGovern A, Orozco G, *et al.* Capture Hi-C reveals novel candidate genes
276 and complex long-range interactions with related autoimmune risk loci. *Nat Commun*
277 2015;**6**:10069. doi:10.1038/ncomms10069
- 278